buildings

MDPI

Article

Mechanical and Microstructural Properties of Ultra-High Performance Concrete with Lightweight Aggregates

Hani Alanazi [1], Oussama Elalaoui [1,2], Musa Adamu [3,4,*], Saleh O. Alaswad [5], Yasser E. Ibrahim [3,*], Aref A. Abadel [6] and Abdulrahman Fahad Al Fuhaid [7]

[1] Department of Civil and Environmental Engineering, College of Engineering, Majmaah University, Al-Majmaah 11952, Saudi Arabia
[2] Civil Engineering Department, National Engineering School of Tunis, University of El Manar, Tunis Belvedere, Tunis 1002, Tunisia
[3] Engineering Management Department, College of Engineering, Prince Sultan University, Riyadh 11586, Saudi Arabia
[4] Department of Civil Engineering, Bayero University Kano, Kano 700223, Nigeria
[5] Nuclear Science Research Institute (NSRI), King Abdulaziz City for Science and Technology (KACST), Riyadh 11442, Saudi Arabia
[6] Department of Civil Engineering, College of Engineering, King Saud University, P.O. Box 800, Riyadh 11421, Saudi Arabia
[7] Department of Civil and Environmental Engineering, College of Engineering, King Faisal University (KFU), P.O. Box 380, Al-Ahsa 31982, Saudi Arabia
* Correspondence: madamu@psu.edu.sa (M.A.); ymansour@psu.edu.sa (Y.E.I.)

Abstract: Although ultra-high-performance concrete (UHPC) presents superior mechanical properties and durability compared to conventional concrete; its spalling resistance to elevated temperatures is much lower compared to conventional concrete due to the high compactness and absence of capillary pores. This paper investigated the influence of lightweight aggregate (LWA) on the strength properties and microstructure of UHPC to enhance its resistance to elevated temperatures. UHPC specimens prepared with LWA as a partial replacement of silica sand were produced. The study evaluated the compressive and flexural strengths, failure mode, mass loss, and microstructure of the specimens, using SEM. The results showed that the compressive strength of the UHPC specimen was reduced with increasing the content of LWA at ambient temperature, but the compressive strength of the UHPC specimens prepared with LWA improved when exposed to elevated temperatures. The replacement of 10% of the silica sand with LWA led to an increase in the compressive strength from 100 MPa to 110 MPa after exposure to 200 °C; however, the flexural strength decreased from 23.6 MPa to 18.3 MPa. On the contrary, the flexural strength of UHPC increased with the inclusion of LWA at an ambient temperature but reduced with high-temperature exposure. The failure mode of UHPC was not significantly affected by the variation in LWA content and temperature. In addition, the SEM result confirms that LWA is an effective internal curing material for enhancing the microstructure and compressive strength of UHPC

Keywords: UHPC; lightweight aggregate; silica sand; elevated temperature; internal curing

Citation: Alanazi, H.; Elalaoui, O.; Adamu, M.; Alaswad, S.O.; Ibrahim, Y.E.; Abadel, A.A.; Al Fuhaid, A.F. Mechanical and Microstructural Properties of Ultra-High Performance Concrete with Lightweight Aggregates. *Buildings* **2022**, *12*, 1783. https://doi.org/10.3390/buildings12111783

Academic Editor: Ahmed Senouci

Received: 29 September 2022
Accepted: 19 October 2022
Published: 24 October 2022

1. Introduction

Sustainable development is becoming popular globally, which has led to the development of various systems in the construction industry for new technologies. These new technologies come with unique challenges [1,2]. Ultra-high-performance concrete (UHPC), also known as reactive powder concrete, is a new cementitious composite characterized by excellent mechanical properties and durability performance [3–5]. However, UHPC is also characterized by a low water to binder (w/b) ratio that can cause a low degree of cement hydration, specifically less than 50%. The UHPC matrix may contain a

significant quantity of unhydrated cement particles, which essentially do not participate in the development of hardening properties. This low w/b ratio is responsible for a remarkable autogenous shrinkage in UHPC, which can lead to cracking [6,7]. Moreover, self-desiccation raises the pore water capillary tension, resulting in autogenous shrinkage [8]. Therefore, supplying more water is vital to speed up the cement hydration process, leading to a decrease in self-desiccation. However, due to the high impermeability of the UHPC mixture, the external water-curing technique could be inefficient because of the difficulty for external curing water to permeate the UHPC matrix and participate in cement hydration [9]. Thus, internal curing, which is a reliable method for providing additional water to cure concrete composites prepared with a low w/b ratio, could be the best alternative [10–12]. As a result of internal curing, tremendous benefits have been achieved, including a reduction in the shrinkage of high-performance cement composites [13,14], improved compressive strength [13,15], decreased potential cracks [14,16], and improved durability [17]. According to Bentz, Lura [18], the inclusion of a small amount of internal curing agents, which can be effectively dispersed in the matrix, is more effective than using a large amount of internal curing agents in reserving water at the point of mixing and setting of cement composites, and then gradually discharging the water for internal curing. The method adopted by De la Varga and Graybeal [19] provides internal curing by using pre-saturated lightweight aggregate (LWA) to noticeably reduce the autogenous shrinkage of cementitious materials. However, previous studies on UHPC utilizing internal curing showed a trade-off between hardened properties and autogenous shrinkage of concrete when a superabsorbent polymer or rice-husk ash was used [20,21].

LWAs are commonly used in the production of high-strength lightweight concrete (HSLC) for structural purposes. Due to the pores in the LWAs, the weight of the HSLC mixture is 20–40% less than that of ordinary concrete [22]. Meng and Khayat [21] investigated the efficiency of internal curing using various dosages of lightweight sand (LWS) in the UHPC matrix. The results indicated that replacing 25% of the volume of LWS resulted in the highest strength. However, the elastic modulus of UHPC was reduced with LWS. This behavior was consistent with the findings observed in high-performance concrete [23]. In addition, several studies have been carried out to determine the performance of UHPCs internally cured with LWAs, as indicated in the previous literature, which contains: expanded shale [24]; prewetted calcined bauxite [25]; porous calcined bauxite [13]; pumice [26]; and porous ceramic fine aggregate [27]. However, a reduction in strength was observed compared to the control mixture in some UHPC. Some studies with properly designed internal curing agents showed a slightly higher strength was obtained and did not account for elastic modulus. Golias, Castro [28] reported that for a properly designed mixture proportion to take care of the absorbed water by the LWA before cement setting, LWA could guarantee a desirable internal curing effect in concrete composites. Liu and Wei [13] and Liu and Wei [29] discovered that calcined bauxite-aggregate blended in an air-dry condition could absorb water during mixing and discharge it into the concrete mixture after setting, revealing the ability of calcined bauxite aggregate to provide internal curing in the UHPC mixture. However, various methods of providing water for internal curing in the UHPC matrix have been reported in the past literature [25,30,31]. Nevertheless, the widely used methods are extra internal curing water for pre-wetting or introducing dry agents with the introduction of internal curing water while mixing. In contrast, other approaches keep the same total amount of water as the control mixture. Shen, Lu [32] explored the role of the physicochemical properties of LWA in controlling the strength development of UHPC. The review of the literature showed that inclusion of LWA in UHPC mixtures enhanced the overall macroscale properties. Thus, incorporating LWAs into UHPC system is expected to influence its resistance to elevated temperatures. Based on a review of the literature mentioned above, there are limited studies on the mechanical properties and microstructure of UHPC at elevated temperatures incorporating LWAs.

Concrete subjected to a high temperature is prone to spalling, and the risk of concrete spalling when exposed to elevated temperatures is affected by several factors. These factors include concrete materials, type of aggregate, aggregate size, specimen dimension, rate of heating, loading condition, and test method [33]. Despite its exceptional mechanical properties and urability, UHPC is more vulnerable to explosive spalling compared to ordinary concrete exposed to elevated temperatures [34,35]. Bažant and Thonguthai [36] and Kodur [35] defined the process of explosive spalling at high temperatures. It was suggested that in UHPC mixtures, explosive spalling occurs due to the accumulated extremely high pore pressure. Therefore, the UHPC's denser microstructures cause the formation of internal water vapor pressure at very high temperatures; thus, the chance of explosive spalling in UHPC increases with the decrease in porosity due to the low w/b ratio [37]. Additionally, Phan and Carino [38] evaluated explosive spalling of high-performance concrete subjected to a temperature of 200–235 °C as a result of thermal stress and internal pore pressure. Yi [37] reported the explosive spalling of UHPC at a temperature in the range of 400–500 °C for 10 min of heating. Richard and Cheyrezy [39] observed the reduction in free water in UHPC at elevated temperatures between 230 °C and 250 °C. This phenomenon was explained by the potential accumulation of crystal hydrate and xonotlite, which enhanced the pozzolanic reaction completion level to 95% at elevated temperatures compared to 72% level at room temperature; thus, leading to a denser microstructure of the UHPC. Zheng, Li [40] analyzed the effect of elevated temperature (20 to 800 °C), specimen size, and fiber content on the compressive strength and microstructure of UHPC. The result indicates the progressive increase in compressive strength up to 400 °C temperature exposure and then a systematic decrease in strength at elevated temperatures above 400 °C. Liu and Huang [41] and Tai, Pan [42] reported an improved strength with an increase in temperature up to 300 °C, and then reduced compressive strength above 300 °C temperature exposure. Based on a review of the literature mentioned above, there are limited studies on the mechanical properties and microstructure of UHPC at elevated temperatures incorporating LWAs.

Over the past few decades, researchers have carried out numerous studies on the development of UHPC mixtures by incorporating some additives to achieve mechanically superior and durable UHPC when exposed to adverse conditions [43,44]. The effect of incorporating some admixtures to the UHPC matrix, which includes steel fiber [45], polypropylene, steel fiber [46,47], and steel slag [48], was investigated recently. However, limited studies can be found that deal with the exposure of UHPC mixtures to elevated temperatures. Thus, this study aimed to investigate the mechanical properties and microstructure of UHPC mixtures containing LWAs at elevated temperatures. A UHPC matrix incorporated with different dosages of LWA was considered for evaluating the effect of elevated temperature and LWA content on the compressive and flexural strengths of the UHPC mixture. In addition, scanning electronic microscopy (SEM) was performed on the UHPC mixture before and after temperature exposure.

2. Experimental Program

2.1. Materials

Ordinary Portland cement type I and silica fume locally produced by Sika KSA (Sika Fume HR) were used together as a binder in preparing UHPC mixes (Figure 1). The chemical compositions of the cement and silica fume are presented in Table 1. The specific surface area of the silica fume was 18 m^2/g. Unwashed silica sand with a maximum size of 1.18 mm, fineness modulus of 2.3, and a specific surface area of 3550 cm^2/g was used in this study. The sand was sourced from a quarry site around Riyadh, Saudi Arabia. Steel fibers with hooked ends were considered with 1% volume fractions. The fiber has an aspect ratio of 40, a diameter of 1.0 mm, and a tensile strength ranging between 800 and 1500 MPa. The physical and mechanical properties of the fiber are listed in Table 2. In order to achieve high flowability with a relatively low dosage, a polycarboxylic ether-based polymer (MasterGlenium-Trade name) was used as a superplasticizer.

(**a**) (**b**) (**c**) (**d**) (**e**)

Figure 1. Materials used in the preparation of UHPC mix. (**a**) Steel fiber. (**b**) Silica fume. (**c**) White sand. (**d**) Cement. (**e**) Superplasticizer.

A single-size fine LWA free from impurities that might interfere with the setting and hardening of the binder was used. The aggregate originated from a volcanic tuff of scoria available on the outskirts of Al-Madina, Saudi Arabia. The nominal size and absolute density of the fine aggregate were 5 mm and 2.929 g/cm^3, respectively. The single size was selected in order to ensure uniform flowability and dispersion within the matrix, which is difficult to achieve with graded aggregate, given the reduced quantity of water used in UHPC.

Table 1. Chemical compositions of cement and silica fume.

Chemical Composition (%)	Cement	Silica Fume
SiO_2	22.52	94
Al_2O_3	5.80	0.21
Fe_2O_3	3.52	0.09
SO_3	2.54	-
CaO	62.08	0.12
MgO	1.55	0.33
Na_2O	0.05	-
K_2O	0.56	0.38
L.O.I	0.94	1.2

Table 2. Physical and mechanical properties of steel fibers.

Diameter (μm)	Length (mm)	Aspect Ratio	Tensile Strength (MPa)	Density (g/cm^3)	Elastic Modulus (GPa)
200	19.5	97.5	2500	7.8	200

2.2. Specimen Preparation and Mixture Proportion

Four different mixtures of UHPC of a constant water–binder ratio of 0.2 and varying proportions (0–15%) of LWA partially replacing silica sand were produced. The mix proportions of the mixtures are shown in Table 3. The specimens were labeled with the letter "L" and a number. The number represents the percentage of LWA in the mixture.

A planetary mixer was used to mix the mixtures. The powdery ingredients, which include cement, silica fume, silica sand, and LWA, were first mixed in the mixer at a low speed for 3 min. Thereafter, water and superplasticizer were introduced, and the mixing continued for another 2 min until the mixture changed to a viscoplastic liquid. Finally, fibers were added to the mixture and mixed for an additional 3 min at a high speed. Superplasticizer was added again to ensure better dispersion of fibers and to achieve proper rheological properties of the mixture.

Immediately after mixing, the mixtures were poured into different molds to fabricate specimens needed for compressive and flexural strength tests. All filled molds were then covered with plastic film and kept suspended in the air at a room temperature of 23 °C ± 3 °C for 24 h. After demolding, the specimens were cured in water for 28 days before testing. Cylindrical molds (Ø50 mm × 100 mm) and prisms (40 × 40 × 160 mm) were used for compressive strength and flexural strength tests, respectively. For each test and each mix, four samples were prepared and tested, and the average values reported

Table 3. Proportions of the mixtures used (g).

Mixture Type	Binder		Water	Aggregates		Superplasticizer	Steel Fiber
	Cement	Micro Silica		LWA	Silica Sand		
L0	2646	650.18	617.4	0	2911.9	88.2	231.82
L5	2646	650.18	617.4	145.6	2766.13	88.2	231.82
L10	2646	650.18	617.4	291.19	2620.56	88.2	231.82
L15	2646	650.18	617.4	436.75	2474.95	88.2	231.82

2.3. Thermal Treatment of the Specimens

In order to examine the influence of elevated temperatures on the UHPC, the specimens (cylinders and prisms), after 28 days of curing, were exposed to 100 °C and 200 °C temperatures at a heating rate of 10 °C/min in an electric furnace. The holding time for the specimens at each temperature was 2 h. The specimens were then allowed to cool to ambient temperature in the furnace before being tested.

2.4. Test Methods

The slump flow test was carried out on the different fresh mixes based on the ASTM C143/C143M [49]. A standard-truncated cone with an internal Ø 200 mm at the base, Ø 100 mm at the top, and 300 mm height was used. The flow was measured as the averaged diameters of the circular-spreading concrete. The compressive strength test was carried out in accordance with ASTM C109/C109M [50] while the three-point loading technique was used for the flexural strength test following the ASTM C78/C78M [51] protocol. Four (4) replicates for each specimen type and property were tested and averaged. The strength tests were conducted using an electromechanical testing machine type NL 42564 under load control at a rate of 5 kN/s accurately maintained until the load indicator showed a decreasing trend and the specimens displayed a well-defined fracture pattern. The fracture patterns of each specimen were physically observed to identify the mode of failure of the various specimens. Furthermore, mass loss of the specimens, expressed in percentage, was determined by measuring the mass of the specimens before and after exposure to temperatures.

For the microstructure analysis, some selected specimens were examined using SEM. The remnant specimens obtained from the compressive strength test were utilized for SEM. Before the test, the specimens were oven dried at 60 °C until a constant mass was achieved to stop further hydration.

3. Results and Discussion

3.1. Flowability of UHPC

The results of the workability of the UHPC mixes measured using the flowability test are shown in Figure 2. The flowability was found to increase with the increment in partial replacement of the sand with LWA. The improvement in the flowability can be attributed to the lower water absorption of the LWA in comparison to the sand it replaced. Therefore, when the LWA was added, the further absorption of the mixing water by the sand is reduced; this gives the mixture more water to achieve consistency.

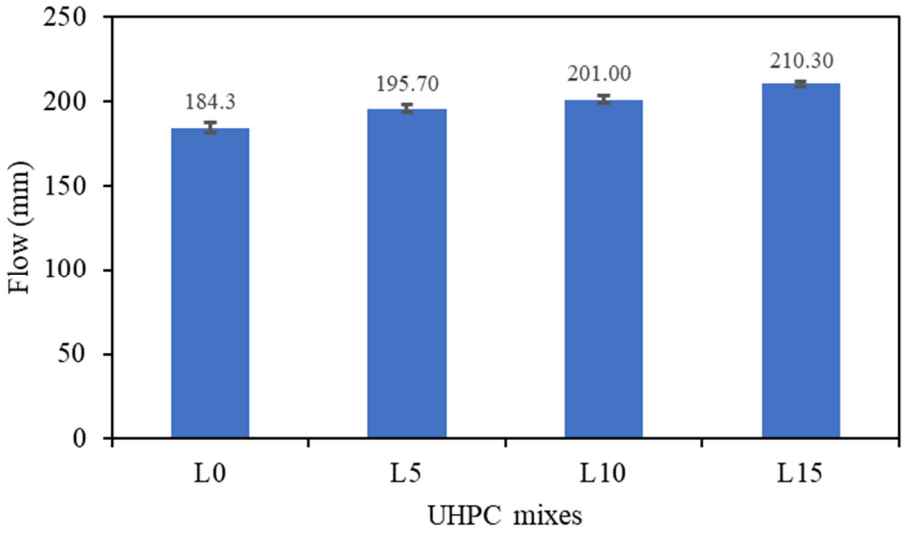

Figure 2. Flow characteristics of UHPC mixtures.

3.2. Mass Loss

The reduction in mass of the UHPC specimens heated at 100 and 200 °C is depicted in Figure 3. The mass loss, expressed in percentage, was determined as the quotation of the mass of the specimen before and after heating. Clearly, all of the specimens suffered a mass reduction. The magnitude of the loss intensified with the temperature increase and rising content of LWA. At 100 °C, the mass losses of specimens L0 and L15 were 0.61% and 0.96%, while at 200 °C, the values rose to 2.95% and 4.19%, respectively. The mass loss experienced by the specimens can be attributed to the escape of evaporated water contained in the specimens, which occurs more with the growing content of LWA [13].

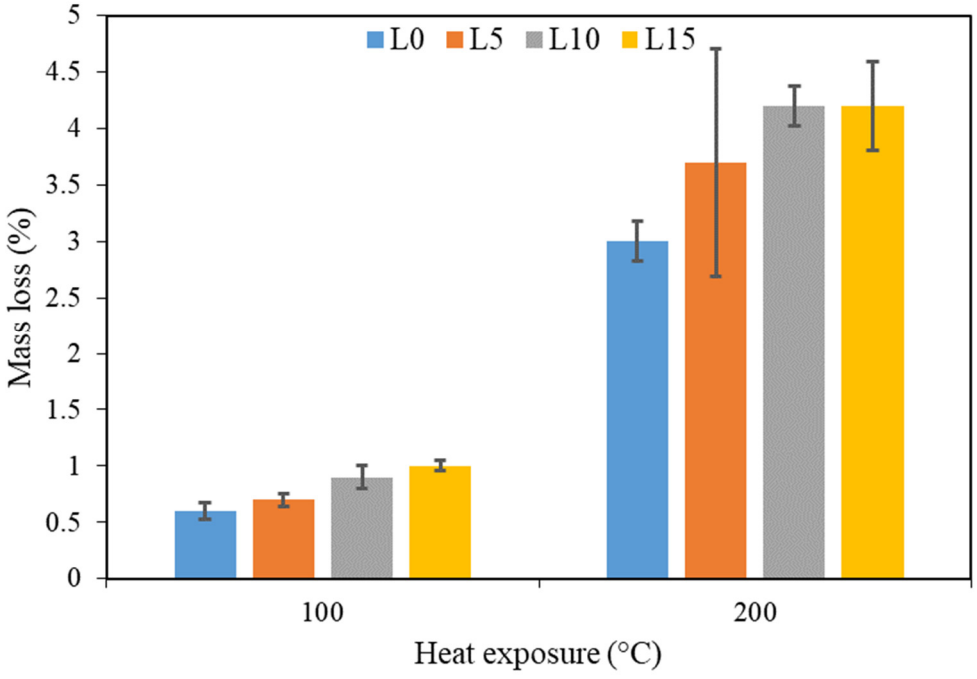

Figure 3. Percentage of mass loss after heat exposure.

3.3. Compressive Strength

The compressive strengths of the UHPC specimens containing different percentages of LWA exposed to different temperatures are shown in Figure 4. At an ambient temperature, it can be seen that the compressive strength of the UHPC specimen improved with a low content of LWA (5%) but decreased with the increasing content of LA. However, after exposure to elevated temperatures, generally, the compressive strengths of all of the specimens increased due to the autoclaving effect that allows for further hydration. This implies that elevated temperatures up to 200 °C improve the compressive strength development of UHPC which incorporates LWA. However, the improvement is more pronounced at 100 °C. The specimens with a higher content of LWA displayed better strength retention as the temperature increased after exposure to elevated temperatures. Only the specimens containing LWA showed a higher compressive strength compared to the specimens without LWA after exposure to 200 °C. This finding is in agreement with that of Tai, Pan [42] that reported that the compressive strength of UHPC improved with exposure to up to 300 °C temperatures. Similarly, the improved strength was equally observed with the incorporation of calcined bauxite as a partial replacement of silica sand in UHPC [13,29].

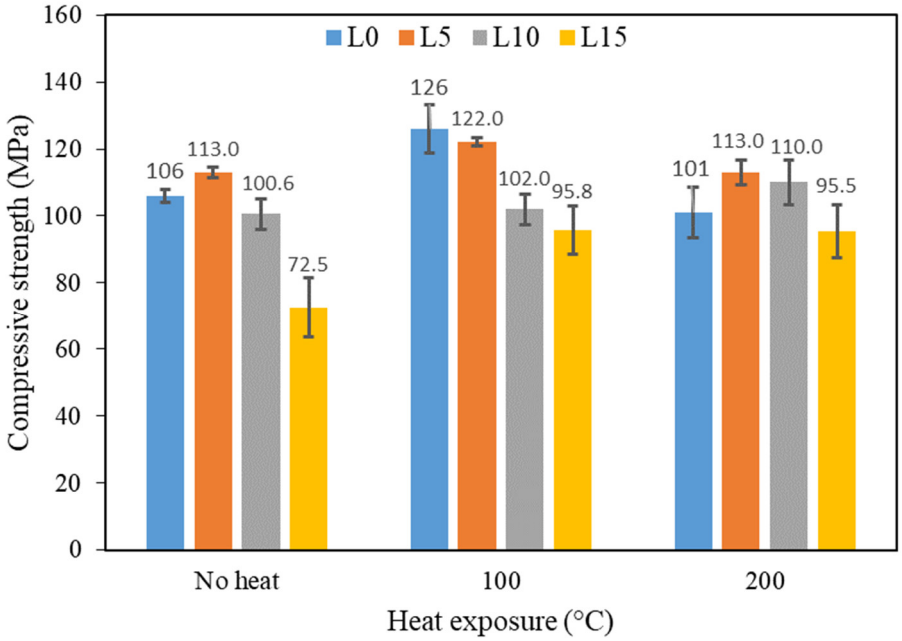

Figure 4. Compressive strength of UHPC mixes.

3.4. Flexural Strength

The flexural strengths of the UHPC specimens exposed to ambient and elevated temperatures are presented in Figure 5. It is apparent that, at ambient temperature, the flexural strength of the specimens increased with the addition of LWA. The strength improvement may be related to the release of water from LWA which facilitates the continuous hydration process in the matrix. The continuous hydration process, in turn, prevents the propagation of microcracks [52]. However, contrary to the compressive strength results, flexural strength reduction can be noticed with the exposure of the specimens to elevated temperatures. This indicates that an elevated temperature has a devastating effect on the flexural strength of the UHPC. The conversion of reserved water in LWA to vapor leads to thermal pressure build-up that consequently induces microcracks, which are responsible for the reduction in flexural strength of UHPC at elevated temperatures [47]. This finding is in agreement with that of He, Du [52].

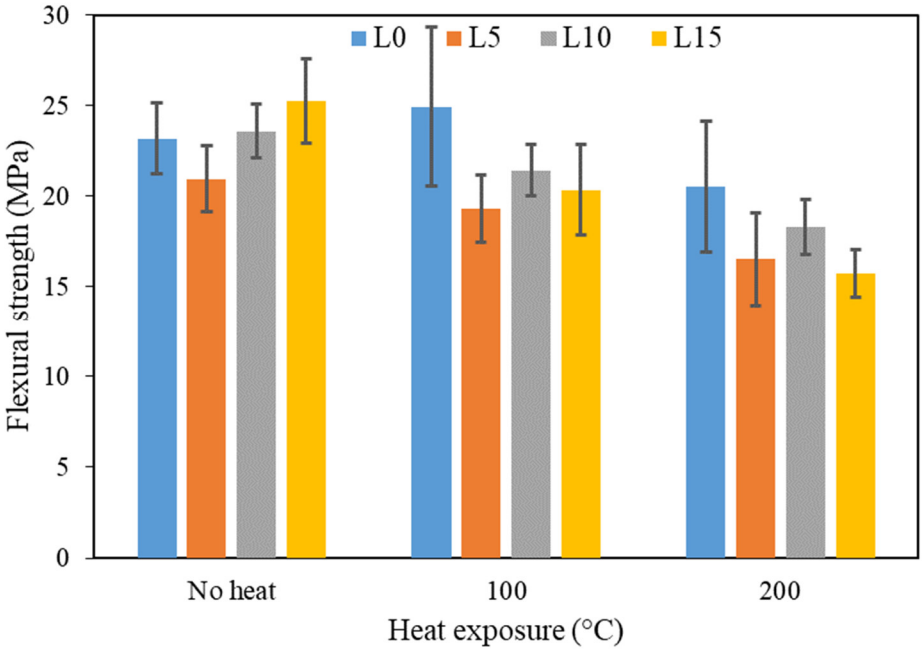

Figure 5. Flexural strength of UHPC mixes.

3.5. Failure Mode of UHPC

Figure 6 shows the failure patterns of the various UHPC specimens after the compression test. All of the specimens virtually manifested the same pattern of failure, irrespective of their LWA content and exposed temperatures. However, during the test, small chips of the specimens at the top and bottom started to fly off. This chipping continued until a larger chip exited the top and bottom of the cylinder before the specimen rapidly failed. This demonstrated a high degree of brittleness which is typical for high-strength materials [53]. This behavior is different from that of conventional concrete, where visible cracks start to appear at the top and gradually spread and enlarge with increased compressive load before rapidly failing. These result findings were in agreement with those of Gu [54].

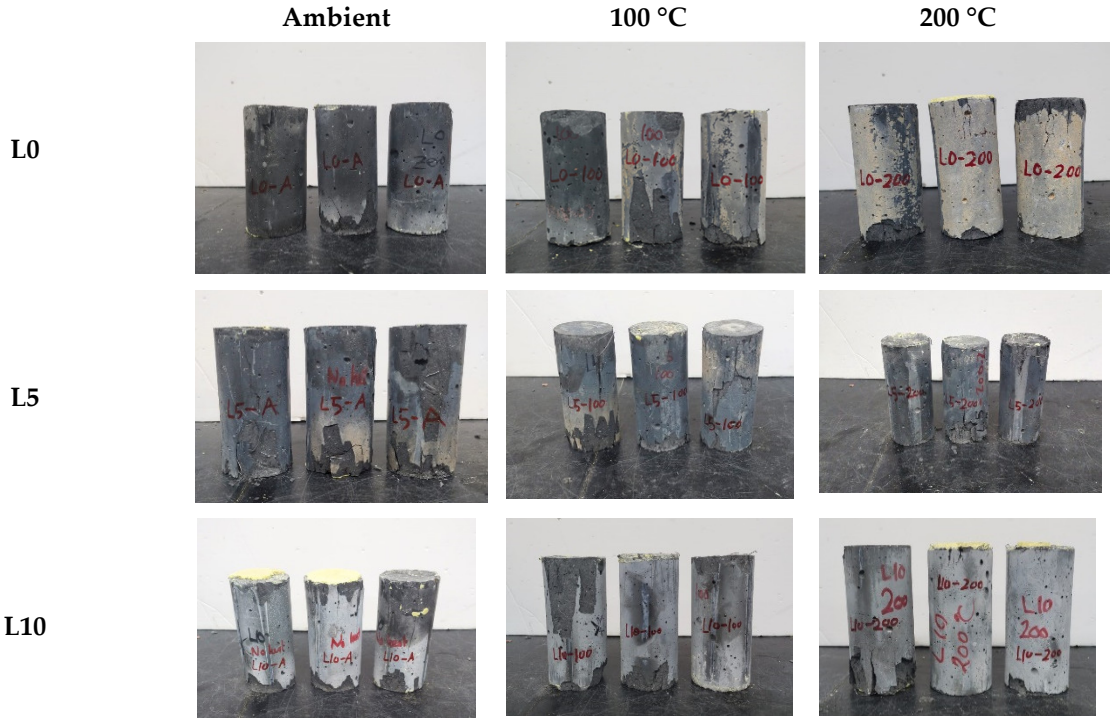

L15

Figure 6. Failure patterns.

3.6. Microstructural Analysis

Figures 7 and 8 represent the SEM micrograms of unheated and heated UHPC specimens containing 0 and 15% LWA at different magnifications. SEM is generally accepted as a useful technique for evaluating the microstructure of UHPC [52,55]. It can be observed that the internal microstructure of the unheated UHPC containing no LWA (Figure 7a,b) mostly consists of hydration products, unhydrated cementitious materials particles, aggregates, pores, and air voids. The main hydration products identified are calcium silicate hydrate gels and calcium hydroxide crystals. Furthermore, the interface between the aggregate and matrix is found to be as compact as the bulk cement paste phase. Owing to the exposure of the specimen to heating, the specimens relatively exhibited a more homogeneous microstructure than the unheated specimen as shown in Figure 7c,d. The homogeneity is paramount for the improved performance of UHPC.

For the unheated specimens containing LWA (L15), as depicted in Figure 8a,b, the microstructure seems denser than the unheated specimen without LWA (L0). Voids and cracks are less visible and the microstructure of the paste, as well as at the interface between aggregate and paste, appeared more uniformly distributed. The improved microstructure is due to the continuous hydration process trigged by the supply of more water reserved in the LWA, which confirms the effectiveness of the LWA as internal curing material [13,56]. Despite the improved microstructure, the strong performance of the specimen with LWA (L15) is, however, inferior to that of the specimen without LWA (L0). This is a possible phenomenon following the intrinsic weakness of LWA, due to its high porosity, which has a significant bearing on the strength-reduction effect of concrete, especially when present in a reasonable quantity [57]. Nonetheless, upon heating, the specimen (L15-200) as presented in Figure 8c,d exhibited better microstructure enhancement which explained the improved compressive strength of the specimen compared to the unheated one. This signified that an elevated temperature is useful for improving the microstructure and compressive strength of UHPC containing LWA.

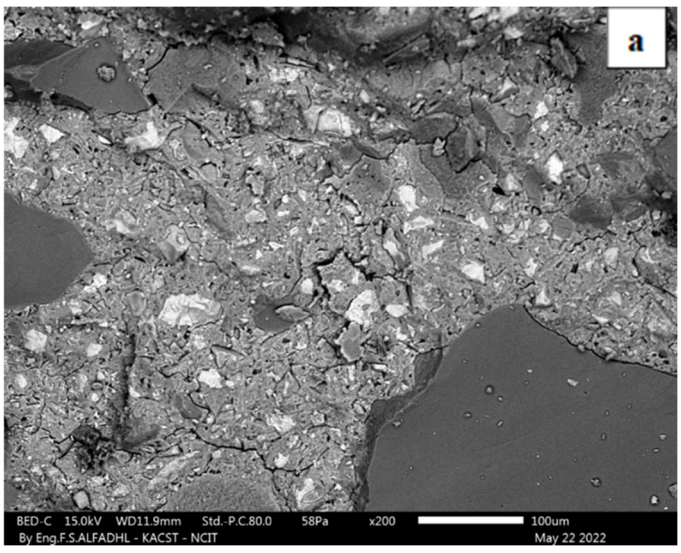

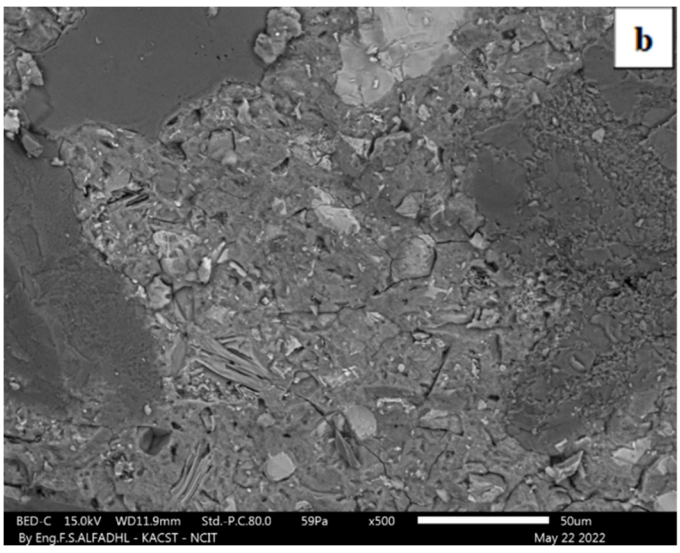

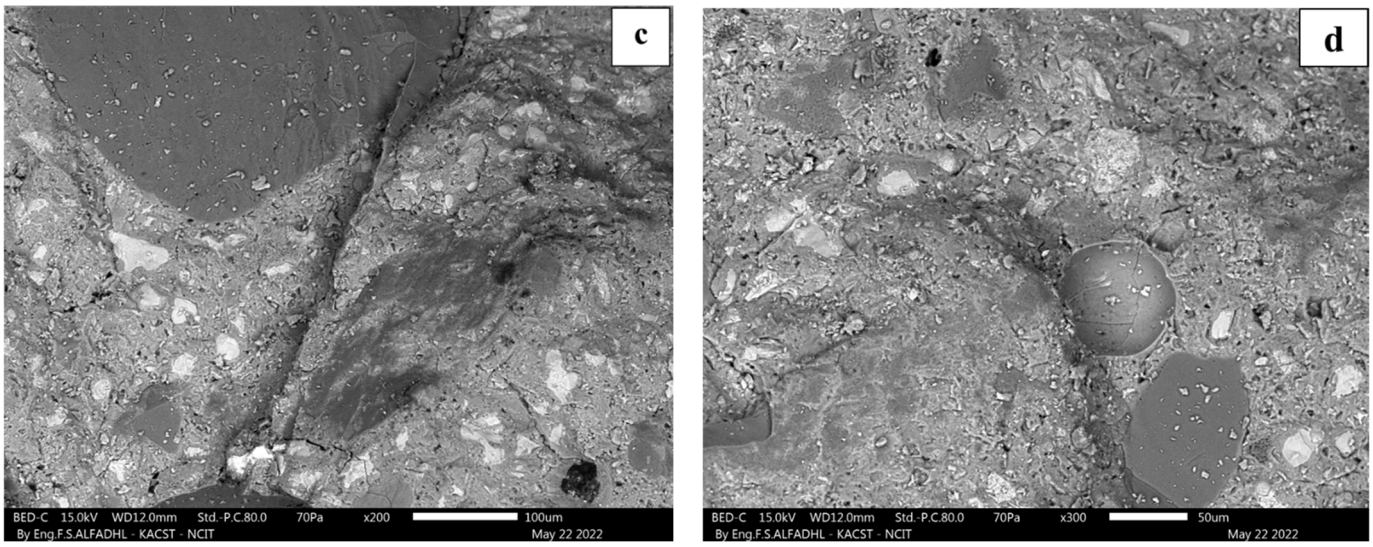

Figure 7. Microstructural SEM images of UHPC-L0: (**a**) ambient at 200× magnification; (**b**) ambient at 500× magnification; (**c**) 200 °C at 200× magnification; and (**d**) 300 °C at 300× magnification.

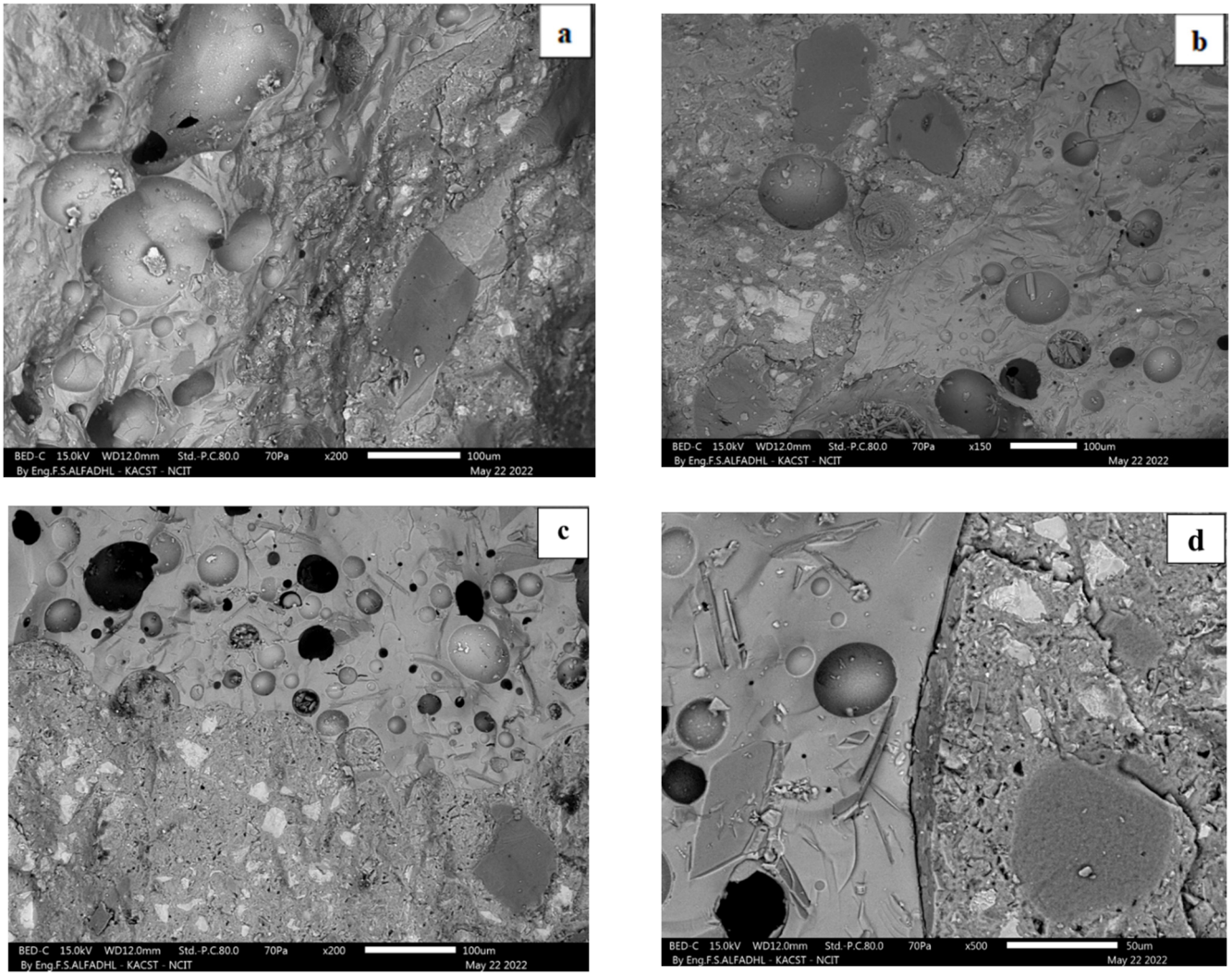

Figure 8. Microstructural SEM images of UHPC-L15: (**a**) ambient at 200× magnification; (**b**) ambient at 150× magnification; (**c**) 200 °C at 200× magnification; and (**d**) 200 °C at 500× magnification.

4. Conclusions

In this study, the influence of incorporating LWA into UHPC mixtures to enhance its spalling resistance when exposed to elevated temperatures was explored by investigating the mechanical properties and microstructure, and the following conclusions were drawn:

(1) The compressive strength of UHPC improves with a low content (5%) of LWA but reduces with a high content (>5%) at ambient temperature. However, with the temperature increased to 200 °C, improved compressive strength can be achieved even with 15% LWA. Increasing the content of LWA resulted in a better retention of the compressive strength as the temperature increased to 200 °C. The replacement of 10% and 15% of silica sand by LWA increased the compressive strength from 100 MPa to 110 MPa and from 72.5 MPa to 95.5 MPa, respectively, after exposure to 200 °C. No change was observed for specimens containing 5% LWA after exposure to 200 °C, while the compressive strength of specimens prepared without LWA decreased from 106 MPa to 101 MPa after exposure to 200 °C;

(2) Flexural strength of UHPC improved with LWA but reduced when exposed to elevated temperatures. The negative influence of incorporating LWA into UHPC mixtures on the flexural strength was higher comparing to its influence on other properties. The replacement of silica sand with 5%, 10%, and 15% of LWA resulted in reducing the flexural strength by 21%, 22%, and 37%, respectively.

(3) Microstructural analysis demonstrated a denser microstructure with fewer microcracks when LWA was incorporated. Effective bonding between the matrix and LWA was observed, which confirms that the LWA is an effective internal curing material for improving the microstructure of UHPC, especially when exposed to elevated temperatures.

(4) The mass loss increased as the content of LWA and temperature increased due to the escape of the evaporated water contained in the specimens. The specimens containing 10% and 15% LWA lost about 4% of their masses after exposure to 200 °C. However, the variation in LWA content and temperatures have an insignificant effect on the mode of failure of UHPC.

Although this study showed the influence of elevated temperatures on the macro mechanical properties and microstructure of UHPC incorporating LWA, further studies are needed to explore the effect of pore sizes of LWAs, saturation levels of LWAs, and the distribution of LWAs in concrete mixtures on the spalling resistance of UHPC exposed to elevated temperatures

Author Contributions: Conceptualization, H.A., O.E., S.O.A. and A.A.A.; methodology, H.A., M.A. and A.F.A.F.; software, H.A., O.E. and A.F.A.F.; validation, H.A., M.A. and Y.E.I.; formal analysis, H.A. and M.A.; investigation, H.A., O.E., S.O.A. and A.A.A.; resources, H.A. and Y.E.I.; data curation, H.A., M.A., S.O.A., and A.F.A.F.; writing—original draft preparation, H.A., O.E., M.A., A.A.A. and M.A.; writing—review and editing, Y.E.I. and A.F.A.F.; visualization, H.A., M.A., and Y.E.I.; supervision, Y.E.I.; project administration, H.A.; funding acquisition, H.A. and Y.E.I. All authors have read and agreed to the published version of the manuscript.

Funding: This research was supported by the Deanship of Scientific Research at Majmaah University for supporting this work under project number R-2022-322. Furthermore, the authors acknowledge the support of Prince Sultan University in paying the article processing charges (APC) of this publication.

Data Availability Statement: Not applicable.

Acknowledgments: The authors would like to thank the Deanship of Scientific Research at Majmaah University for supporting this work under project number R-2022-322 and Structures and Materials laboratory (S&M Lab) of the College of Engineering, Prince Sultan University, Riyadh, Saudi Arabia, for their vital support.

Conflicts of Interest: The authors declare no conflict of interest.

References

1. Hrabova, K.; Teply, B.; Vymazal, T. Sustainability assessment of concrete mixes. *IOP Conf. Ser. Earth Environ. Sci.* **2020**, *444*, 012021.
2. Horňáková, M.; Lehner, P.; Le, T.D.; Konečný, P.; Katzer, J. Durability characteristics of concrete mixture based on red ceramic waste aggregate. *Sustainability* **2020**, *12*, 8890.
3. Meng, W.; Khayat, K.H. Mechanical properties of ultra-high-performance concrete enhanced with graphite nanoplatelets and carbon nanofibers. *Compos. Part B Eng.* **2016**, *107*, 113–122.
4. Abadel, A.A.; Khan, M.I.; Masmoudi, R. Experimental and numerical study of compressive behavior of axially loaded circular ultra-high-performance concrete-filled tube columns. *Case Stud. Constr. Mater.* **2022**, *17*, e01376.
5. Abadel, A.; Abbas, H.; Almusallam, T.; Alshaikh, I.M.; Khawaji, M.; Alghamdi, H.; Salahc, A.A. Experimental study of shear behavior of CFRP strengthened ultra-high-performance fiber-reinforced concrete deep beams. *Case Stud. Constr. Mater.* **2022**, *16*, e01103.
6. Bao, Y.; Valipour, M.; Meng, W.; Khayat, K.H.; Chen, G. Distributed fiber optic sensor-enhanced detection and prediction of shrinkage-induced delamination of ultra-high-performance concrete overlay. *Smart Mater. Struct.* **2017**, *26*, 085009.
7. Bao, Y.; Meng, W.; Chen, Y.; Chen, G.; Khayat, K.H. Measuring mortar shrinkage and cracking by pulse pre-pump Brillouin optical time domain analysis with a single optical fiber. *Mater. Lett.* **2015**, *145*, 344–346.
8. Justs, J.; Wyrzykowski, M.; Bajare, D.; Lura, P. Internal curing by superabsorbent polymers in ultra-high performance concrete. *Cem. Concr. Res.* **2015**, *76*, 82–90.
9. Aïtcin, P.-C. *High Performance Concrete*; CRC Press: Boca Raton, FL, USA, 1998.
10. Bentz, D.P.; Weiss, W.J. *Internal Curing: A 2010 State-Of-The-Art Review*; US Department of Commerce, National Institute of Standards and Technology: Gaithersburg, MD, USA, 2011.
11. Wehbe, Y.; Ghahremaninezhad, A. Combined effect of shrinkage reducing admixtures (SRA) and superabsorbent polymers (SAP) on the autogenous shrinkage, hydration and properties of cementitious materials. *Constr. Build. Mater.* **2017**, *138*, 151–162.
12. Jensen, O.M.; Hansen, P.F. Water-entrained cement-based materials: I. Principles and theoretical background. *Cem. Concr. Res.* **2001**, *31*, 647–654.
13. Liu, Y.; Wei, Y. Internal Curing by Porous Calcined Bauxite Aggregate in Ultrahigh-Performance Concrete. *J. Mater. Civ. Eng.* **2021**, *33*, 04020497.
14. Valipour, M.; Khayat, K.H. Coupled effect of shrinkage-mitigating admixtures and saturated lightweight sand on shrinkage of UHPC for overlay applications. *Constr. Build. Mater.* **2018**, *184*, 320–329.
15. Al-Khaiat, H.; Haque, M. Effect of initial curing on early strength and physical properties of a lightweight concrete. *Cem. Concr. Res.* **1998**, *28*, 859–866.
16. Henkensiefken, R. Internal Curing in Cementitious Systems Made Using Saturated Lightweight Aggregate. Master's Thesis, Purdue University, West Lafayette, IN, USA, 2008.
17. Zhutovsky, S.; Kovler, K. Effect of internal curing on durability-related properties of high performance concrete. *Cem. Concr. Res.* **2012**, *42*, 20–26.
18. Bentz, D.P.; Lura, P.; Roberts, J.W. Mixture proportioning for internal curing. *Concr. Int.* **2005**, *27*, 35–40.
19. De la Varga, I.; Graybeal, B.A. Dimensional stability of grout-type materials used as connections between prefabricated concrete elements. *J. Mater. Civ. Eng.* **2015**, *1107*, 1–10.
20. Khayat, K.H.; Meng, W.; Valipour, M.; Hopkins, M. *Use of Lightweight Sand for Internal Curing to Improve Performance of Concrete Infrastructure*; Missouri. Department of Transportation. Construction and Materials Division: Jefferson City, MO, USA, 2018.
21. Meng, W.; Khayat, K. Effects of saturated lightweight sand content on key characteristics of ultra-high-performance concrete. *Cem. Concr. Res.* **2017**, *101*, 46–54.
22. *BS EN 206-1*; Concrete: Specification, Performance, Production and Conformity. BSI: London, UK, 2000.
23. Schwesinger, P. Reducing Shrinkage in HPC by International Curing Using Pre Soaked LWA. *Control. Crack. Early Age Concr.* **2002**, 333–338.
24. Cao, Y.; Liu, R.; Xu, Y.; Ye, F.; Xu, R.; Han, Y. Effect of SiO2, Al2O3 and CaO on characteristics of lightweight aggregates produced from MSWI bottom ash sludge (MSWI-BAS). *Constr. Build. Mater.* **2019**, *205*, 368–376.
25. Liu, Y.; Wei, Y. Internal curing efficiency and key properties of UHPC influenced by dry or prewetted calcined bauxite aggregate with different particle size. *Constr. Build. Mater.* **2021**, *312*, 125406.
26. Liu, K.; Yu, R.; Shui, Z.; Li, X.; Guo, C.; Yu, B.; Wu, S. Optimization of autogenous shrinkage and microstructure for Ultra-High Performance Concrete (UHPC) based on appropriate application of porous pumice. *Constr. Build. Mater.* **2019**, *214*, 369–381.
27. Ozawa, M.; Parajuli, S.S.; Uchida, Y.; Zhou, B. Preventive effects of polypropylene and jute fibers on spalling of UHPC at high temperatures in combination with waste porous ceramic fine aggregate as an internal curing material. *Constr. Build. Mater.* **2019**, *206*, 219–225.
28. Golias, M.; Castro, J.; Weiss, J. The influence of the initial moisture content of lightweight aggregate on internal curing. *Constr. Build. Mater.* **2012**, *35*, 52–62.
29. Liu, Y.; Wei, Y. Effect of calcined bauxite powder or aggregate on the shrinkage properties of UHPC. *Cem. Concr. Compos.* **2021**, *118*, 103967.

30. Dong, E.; Yu, R.; Fan, D.; Chen, Z.; Ma, X. Absorption-desorption process of internal curing water in ultra-high performance concrete (UHPC) incorporating pumice: From relaxation theory to dynamic migration model. *Cem. Concr. Compos.* **2022**, *133*, 104659.
31. Kazemian, M.; Shafei, B. Internal curing capabilities of natural zeolite to improve the hydration of ultra-high performance concrete. *Constr. Build. Mater.* **2022**, *340*, 127452.
32. Shen, P.; Lu, J.-X.; Lu, L.; He, Y.; Wang, F.; Hu, S. An alternative method for performance improvement of ultra-high performance concrete by internal curing: Role of physicochemical properties of saturated lightweight fine aggregate. *Constr. Build. Mater.* **2021**, *312*, 125373.
33. Mohd Ali, A.; Sanjayan, J.; Guerrieri, M. Specimens size, aggregate size, and aggregate type effect on spalling of concrete in fire. *Fire Mater.* **2018**, *42*, 59–68.
34. Ali, F. Is high strength concrete more susceptible to explosive spalling than normal strength concrete in fire? *Fire Mater.* **2002**, *26*, 127–130.
35. Kodur, V. Fiber reinforcement for minimizing spalling in High Strength Concrete structural members exposed to fire. *Spec. Publ.* **2003**, *216*, 221–236.
36. Bažant, Z.P.; Thonguthai, W. Pore pressure and drying of concrete at high temperature. *J. Eng. Mech. Div.* **1978**, *104*, 1059–1079.
37. So, H.-S.; Yi, J.-B.; Khulgadai, J.; So, S.-Y. Properties of Strength and Pore Structure of Reactive Powder Concrete Exposed to High Temperature. *ACI Mater. J.* **2014**, *111*, 335–345.
38. Phan, L.T.; Carino, N.J. Fire performance of high strength concrete: Research needs. In *Advanced Technology in Structural Engineering, Proceedings of the Structures Congress 2000, Philadelphia, PA, USA, 8–10 May 2000*; American Society of Civil Engineers: Reston, VA, USA, 2000; pp. 1–8.
39. Richard, P.; Cheyrezy, M. Composition of reactive powder concretes. *Cem. Concr. Res.* **1995**, *25*, 1501–1511.
40. Zheng, W.; Li, H.; Wang, Y. Compressive behaviour of hybrid fiber-reinforced reactive powder concrete after high temperature. *Mater. Des.* **2012**, *41*, 403–409.
41. Liu, C.-T.; Huang, J.-S. Fire performance of highly flowable reactive powder concrete. *Constr. Build. Mater.* **2009**, *23*, 2072–2079.
42. Tai, Y.-S.; Pan, H.-H.; Kung, Y.-N. Mechanical properties of steel fiber reinforced reactive powder concrete following exposure to high temperature reaching 800 C. *Nucl. Eng. Des.* **2011**, *241*, 2416–2424.
43. Shareef, A.Y. A Study on Durability Properties of Ultrahigh Performance Concrete (UHPC) Utilizing Local Fine Quartz Sand. Master's Thesis, King Fahd University of Petroleum and Minerals, Dhahran, Saudi Arabia, 2013.
44. Ahmad, S.; Hakeem, I.; Maslehuddin, M. Development of UHPC mixtures utilizing natural and industrial waste materials as partial replacements of silica fume and sand. *Sci. World J.* **2014**, *2014*, 713531.
45. Ahmad, S.; Rasul, M.; Adekunle, S.K.; Al-Dulaijan, S.U.; Maslehuddin, M.; Ali, S.I. Mechanical properties of steel fiber-reinforced UHPC mixtures exposed to elevated temperature: Effects of exposure duration and fiber content. *Compos. Part B Eng.* **2019**, *168*, 291–301.
46. Li, Y.; Zhang, D. Effect of lateral restraint and inclusion of polypropylene and steel fibers on spalling behavior, pore pressure, and thermal stress in ultra-high-performance concrete (UHPC) at elevated temperature. *Constr. Build. Mater.* **2021**, *271*, 121879.
47. Li, Y.; Tan, K.H.; Yang, E.-H. Influence of aggregate size and inclusion of polypropylene and steel fibers on the hot permeability of ultra-high performance concrete (UHPC) at elevated temperature. *Constr. Build. Mater.* **2018**, *169*, 629–637.
48. Liang, X.; Wu, C.; Su, Y.; Chen, Z.; Li, Z. Development of ultra-high performance concrete with high fire resistance. *Constr. Build. Mater.* **2018**, *179*, 400–412.
49. *ASTM C143/C143M*; Standard Test Method for Slump of Hydraulic-Cement Concrete. ASTM International: West Conshohocken, PA, USA, 2012.
50. *ASTM C109/C109M*; Standard Test Method for Comprehensive Strength of Hydraulic Cement Mortars (Using 2-in. or [50-mm] Cube Specimens). ASTM International: West Conshohocken, PA, USA, 2020.
51. *ASTM C78/C78M*; Standard Test Method for Flexural Strength of Concrete (Using Simple Beam with Third-Point Loading). ASTM International: West Conshohocken, PA, USA, 2022.
52. He, Z.-h.; Du, S.-g.; Chen, D. Microstructure of ultra high performance concrete containing lithium slag. *J. Hazard. Mater.* **2018**, *353*, 35–43.
53. Neville, A.M. *Properties of Concrete*; Pearson: Harlow, UK; New York, NY, USA, 2011.
54. Gu, H. Compressive behaviours and failure modes of concrete cylinders reinforced by glass fabric. *Mater. Des.* **2006**, *27*, 601–604.
55. Yu, R.; Spiesz, P.; Brouwers, H. Effect of nano-silica on the hydration and microstructure development of Ultra-High Performance Concrete (UHPC) with a low binder amount. *Constr. Build. Mater.* **2014**, *65*, 140–150.
56. Liu, J.; Shi, C.; Farzadnia, N.; Ma, X. Effects of pretreated fine lightweight aggregate on shrinkage and pore structure of ultra-high strength concrete. *Constr. Build. Mater.* **2019**, *204*, 276–287.
57. Song, M.; Wang, C.; Cui, Y.; Li, Q.; Gao, Z. Mechanical Performance and Microstructure of Ultra-High-Performance Concrete Modified by Calcium Sulfoaluminate Cement. *Adv. Civ. Eng.* **2021**, *2021*, 4002536. https://doi.org/10.1155/2021/4002536.